Room-Temperature Synthesis of Carbonaceous Films of Defined Thickness

Ladislav Kavan,* Karel Micka, and Jaromír Hlavatý

J. Heyrovský Institute of Physical Chemistry, Academy of Sciences of the Czech Republic, Dolejškova 3, CZ-182 23 Prague 8, Czech Republic

Received June 3, 2004. Revised Manuscript Received August 10, 2004

Thin carbonaceous films were prepared on top of a liquid amalgam of alkali metal (Li, Na, K) from gaseous perfluorocyclopentene, perfluorodecalin, perfluoronaphthalene, perfluorobenzene, perfluoro-2-butyne, perfluorohexane, perfluorobiphenyl, perfluorocyclobutane, perfluorocyclohexane, perfluoropyridine, perfluorobenzonitrile, and cyanuric fluoride. All the mentioned precursors are quantitatively dehalogenated by the alkali metal amalgam to give a composite film containing n-doped carbon with the interspersed alkali metal fluoride. The carbonaceous products from perfluoropyridine and cyanuric fluoride contain nitrogen, while the N/C proportion is close to that in the precursor. The kinetics of film growth was rationalized in terms of the electrochemical process in short-circuited corrosion cell. The presented mechanism of film growth at the gas/liquid interface upgrades the previously suggested model of carbonization of solid fluoropolymers by alkali metal amalgams. The method allows room-temperature growth of self-standing carbon thin films of precisely defined thickness.

1. Introduction

The growth of carbonaceous films by CVD and similar processes has been explored extensively in the past. Carbonaceous films are also accessible via soft-chemical reactions occurring typically at room temperature and pressure, but this subject has been investigated to a much lesser extent.[1] Nevertheless, the topic is challenging because thus-prepared carbons may exhibit unusual structure and properties.[1] In most cases, the solid film grows at the interface of two reactants, which may be solid, liquid, or gaseous. This generates a fundamental question about the growth mechanism if neither of the reactants is soluble in the film. In such a case, one would expect that the first monolayer of products separates both reactants from their "chemical contact", i.e., the interfacial chemistry will not propagate any more. However, there are several examples in which the interfacial film grows in a defined way for a long time, even though there is explicit spatial segregation of reactants. This paradox was first clearly formulated by Jansta and Dousek[2] during investigation of the reaction of solid poly(tetrafluoroethylene) (PTFE) with lithium metal dissolved in liquid mercury (Li-amalgam). Contrary to expectation, the film grew easily at the interface of Li-amalgam and PTFE, while neither Li-amalgam nor PTFE could penetrate through the growing film. The same problem was later addressed by Costello and McCarthy.[3,4] for the reactions of fluoropolymers with benzoin dianion.

Total dehalogenation of perfluorinated hydrocarbons, such as PTFE[1,5] and other fluoropolymers[1,6] with alkali metal (Li, Na, K) amalgams proceeds in 100% yield toward n-doped elemental carbon and the corresponding byproduct, alkali metal fluoride. Alternatively, total dehalogenation of PTFE can be achieved by potassium vapor[7] or electrochemically.[8−10] The defluorination of PTFE by alkali metal amalgams provides the best defined product with respect to the thickness and composition of carbonized layer on PTFE. Jansta and Dousek[11] have first rationalized the properties of the amalgam/PTFE interface in terms of the electrochemical corrosion mechanism,[11] assuming the film behaves as a solid electrolyte with mixed electronic/ionic conductivities.[6] This leads to a general dependence of the carbonized layer thickness, L, on the reaction time, t, as follows:

$$L = \sqrt{\frac{EaM\sigma_e\sigma_i \cdot t}{zF\rho(\sigma_e + \sigma_i)}} = K \cdot t^{1/2} \qquad (1)$$

where E denotes electric potential difference of the corrosion cell, a is geometric factor (thickness ratio of carbonized film vs that of the consumed fluoropolymer),

* Corresponding author. E-mail: kavan@jh-inst.cas.cz.

(1) Kavan, L. *Chem. Rev.* **1997**, *97*, 3061.
(2) Jansta, J.; Dousek, F. P. *Electrochim. Acta* **1973**, *18*, 673.
(3) Costello, C. A.; McCarthy, T. J. *Macromolecules* **1987**, *20*, 2819.
(4) Costello, C. A.; McCarthy, T. J. *Macromolecules* **1984**, *17*, 2940.
(5) Kavan, L.; Dousek, F. P.; Janda, P.; Weber, J. *Chem. Mater.* **1999**, *11*, 329.
(6) Kavan, L.; Dousek, F. P.; Micka, K. *Solid State Ionics* **1990**, *38*, 109.
(7) Liang, T. T.; Yamada, Y.; Yoshizawa, N.; Shiraishi, S.; Oya, A. *Chem. Mater.* **2001**, *13*, 2933.
(8) Yasuda, A.; Kawase, N.; Mizutani, W. *J. Phys. Chem. B* **2002**, *106*, 13924.
(9) Amatore, C.; Combellas, C.; Kanoufi, F.; Sella, C.; Thiébault, A.; Thouin, L. *Chem. Eur. J.* **2000**, *6*, 820.
(10) Combellas, C.; Kanoufi, F.; Mazouzi, D.; Thiébault, A. *J. Electroanal. Chem.* **2003**, *556*, 43.
(11) Dousek, F. P.; Jansta, J. *Electrochim. Acta* **1975**, *20*, 1.

10.1021/cm049116a CCC: $27.50
Published on Web 09/25/2004

M is molecular weight of the fluoropolymer unit, z is the number of electrons per fluoropolymer unit, F is Faraday constant, ρ is fluoropolymer density, σ_e and σ_i are the electronic and ionic conductivities, respectively, of the layer, and K is a rate constant.[1,6] In all fluoropolymer/amalgam systems, the ionic conductivity relates to the alkali metal cations. Since $\sigma_i \ll \sigma_e$ the rate constant K is practically controlled by the transport of alkali cations only.

Analogous total dehalogenation of low-molecular-weight fluorocarbons, viz. perfluorobenzene and perfluorohexane, was first reported in 1988, but the kinetic analysis of the film growth failed owing to mechanical instability of the film.[12] Subsequent study of perfluorocyclopentene, perfluoronaphthalene, and perfluorodecalin was motivated by a trail to synthesize C_{60} (fullerene) according to the following hypothetic reactions:[13]

$$12C_5F_8 + 96M_{(Hg)} \rightarrow C_{60} + 96MF \quad (2a)$$

$$6C_{10}F_8 + 48M_{(Hg)} \rightarrow C_{60} + 48MF \quad (2b)$$

$$6C_{10}F_{18} + 108M_{(Hg)} \rightarrow C_{60} + 108MF \quad (2c)$$

(M = akali metal; $M_{(Hg)}$ = alkali metal amalgam). A small amount of C_{60} was, indeed, found in the products of reactions 2a−2c together with carbon nanotubes and spheroidal nanocarbon grains.[13] This is reminiscent of the production of C_{60} by the reaction of potassium with perchlorocyclopentadiene[14] and production of carbon nanotubes via reaction of potassium with tetrachloroethylene[15] or hexachlorobenzene.[16]

Kinetic analysis of the reactions 2a−2c surprisingly revealed that eq 1 is valid for Na amalgam, but not for Li amalgam, where the $L(t)$ scaled linearly with time.[13] Such a behavior of Li amalgam was later confirmed for other precursors, viz. perfluorocyclobutane, perfluorocyclohexane, perfluorobenzene, perfluorobenzonitrile, and perfluoropyridine, but not for perfluoro-2-butyne, where eq 1 was again valid.[17] This work is aimed at obtaining a deeper understanding of the reaction of gaseous low-molecular-weight fluorocarbons with Li, Na, and K amalgams.

2. Experimental Section

Perfluorocyclopentene, perfluorodecalin, perfluoronaphthalene, perfluorobenzene, perfluoro-2-butyne, perfluorohexane, perfluorobiphenyl, perfluorocyclobutane, perfluorocyclohexane, perfluoropyridine, perfluorobenzonitrile, and cyanuric fluoride were purchased from FLUOROCHEM, Ltd. UK, ABCR, GmbH FRG, and Aldrich. (Sometimes, products from different suppliers were tested in comparative runs). Li, Na, and K (from BDH) were dissolved in polarographic grade mercury to a concentration of 0.9−1.3 at. %. The concentration of amalgam was determined by acidimetric titration.

Warning: the dissolution of alkali metals in mercury produces considerable heat. The work is also hazardous owing to flammable (Li, Na, K) and toxic (Hg) reactants.

The perfluorinated precursor (ca. 2−5 g) was first dried by shaking it with ca. 10 mL of the saturated M amalgam, and then distilled. All operations were carried out in evacuated (<1 mPa) all-glass apparatus. The reaction was triggered by opening a breakable glass joint by a magnetic projectile, while the saturated vapor of perfluorinated reactant contacted the surface of liquid alkali metal amalgam (ca. 10−20 mL). The reaction was always carried out with an excess of the perfluorinated hydrocarbon in the vapor phase. Total consumption of the alkali metal manifested itself by no more blackening of the freshly exposed surface of mercury after cracking of the carbonaceous film by shaking. The completeness of the reaction was further controlled by acidimetric titration of the remaining mercury for M after reaction. The formed carbonaceous film was then washed with water in air until complete removal of soluble salts, MF and MOH (typically 5 × 300 mL of water). The collected aqueous extracts were evaporated to dryness and analyzed for OH^- (by acidimetric titration), Li^+, Na^+, and K^+ (by atomic absorption spectroscopy), and F^- (by potentiometry with fluoride selective electrode or by spectrophotometry with Zr-alizarine) as described elsewhere.[6] The final carbonaceous material was dried in a vacuum at 150−250 °C and then subjected to elemental analysis. UV−Vis reflectance spectra of the growing film were measured in situ (Ocean Optics 2000 spectrometer, sealable vacuum optical cell, Hellma). The reflectance spectra were measured in 180° backscattering geometry by fiberglass waveguide, while the acquisition of one spectrum took between 10 and 50 ms. The repeated acquisition of spectra in real time and subsequent calculation of film thickness was controlled by OOI-Base and Nanocalc software. The optical cell was positioned in a thermostated bath (water or ethanol), the temperature of which was controlled (±0.1 °C) by an external thermostat or cryostat.

3. Results and Discussion

3.1. Stoichiometry of Dehalogenation. The analysis of reaction mixture and products (see Experimental Section) confirmed that the $M_{(Hg)}$-driven elimination of fluorine from all perfluorinated reactants (C_xF_y) is quantitative:

$$C_xF_y + yM_{(Hg)} \rightarrow xC + yMF \quad (3)$$

However, more detailed inspection showed that the actual consumption of alkali metal, M, was always slightly larger than required for a complete dehalogenation according to eq 3. The superstoichiometric consumption of alkali metal, M, was evaluated by comparing the actual utilization of M (found by the analysis of $M_{(Hg)}$ and the reaction products) with the calculated one (eq 3). The reaction stoichiometry ($RS = M_{found}/M_{calc}$) is quoted in Table 1. This is reminiscent of the same superstoichiometric consumption of $M_{(Hg)}$ in the reactions with fluoropolymers.[1,6] The superstoichiometry of dehalogenation introduces a negative charge to carbon, $C^{\delta-}$ (n-doping), which is compensated by the corresponding cations of alkali metals:

$$C + \delta\,(M^+ + e^-) \rightarrow M_\delta C \quad (4)$$

In the case of fluoropolymers, the doping level, δ, was between 0.05 and 0.45; most usually around 0.2.[1,6] Analogously as in the case of fluoropolymers,[1,6] the product of reaction 4 is quantitatively hydrolyzed

$$M_\delta C + \delta H_2O \rightarrow H_\delta C + \delta MOH \quad (5)$$

Reaction 5 gives the corresponding alkali metal hydroxide which can be determined by acidimetric titration of

(12) Kavan, L.; Dousek, F. P. *J. Fluorine Chem.* **1988**, *41*, 383.
(13) Kavan, L.; Hlavaty, J. *Carbon* **1999**, *37*, 1863.
(14) Lu, J.; Cong, D. F.; Li, Y. J.; Peng, R. F.; Wang, G. W.; Xie, Y. *J. Am. Chem. Soc.* **2004**.
(15) Wang, X.; Lu, J.; Xie, Y.; Du, G.; Guo, Q.; Zhang, S. *J. Phys. Chem. B* **2002**, *106*, 933.
(16) Jiang, Y.; Wu, Y.; Zhang, S.; Xu, C.; Yu, W.; Xie, Y.; Qian, Y. *J. Am. Chem. Soc.* **2000**, *122*, 12383.
(17) Kavan, L. *Mol. Cryst. Liq. Cryst.* **2002**, *386*, 167.

Table 1. Reaction of Perfluorinated Precursors with M Amalgams (M = Li, Na, K)[a]

Precursor	K_{Li} [nm·s^{-1}]	Doping RS [%]	Doping δ	Note/(ref for K_{Li})
C_6F_{14} Perfluorohexane	0.03	110	0.23	ref 17
C_4F_8 Perfluorocyclobutane	0.2	112	0.24	ref 17
C_6F_{12} Perfluorocyclohexane	0.002	109	0.18	ref 17
$C_{10}F_{18}$ Perfluorodecalin	0.5	111	0.20	ref 13
C_5F_8 Perfluorocyclopentene	7	113	0.21	ref 13
C_5F_8 Perfluorocyclopentene	2			0 °C
C_5F_8 Perfluorocyclopentene	0.3			−15 °C
C_6F_6 Perfluorobenzene	0.06	120	0.20	ref 17
$C_{10}F_8$ Perfluoronaphthalene	0.15	124	0.19	ref 17
$C_{10}F_8$ Perfluoronaphthalene	0.2			ref 13
$C_{12}F_{10}$ Perfluorobiphenyl	0.01	120	0.17	this work
C_6F_5CN Perfluorobenzonitrile	5	115	0.13	ref 17
C_5F_5N Perfluoropyridine	1	118	0.18	ref 17
$C_3F_3N_3$ Cyanuric fluoride	0.003	114	0.14	this work
C_4F_6 Perfluoro-2-butyne	(see text)	114	0.21	ref 17

Precursor	K_{Na} [nm·s$^{-1/2}$]	Doping RS [%]	Doping δ	Note/(ref for K_{Na})
C_4F_8 Perfluorocyclobutane	2.9	106	0.12	ref 17
$C_{10}F_{18}$ Perfluorodecalin	5	119	0.34	ref 13
C_5F_8 Perfluorocyclopentene	9.5	111	0.18	ref 17
C_5F_8 Perfluorocyclopentene	9			ref 13
C_5F_8 Perfluorocyclopentene	18			40 °C
$C_{10}F_8$ Perfluoronaphthalene	18[b]	120	0.16	ref 13
C_4F_6 Perfluoro-2-butyne	9	109	0.14	ref 17

Precursor	K_K [nm·s$^{-1/2}$]	Doping RS [%]	Doping δ	
C_5F_8 Perfluorocyclopentene	0.2	108	0.13	this work
$C_{10}F_8$ Perfluoronaphthalene	0.3	118	0.14	this work

[a] Rate constant, K_M (M = Li, Na, K) is quoted at 25 °C unless stated otherwise. RS = reaction stoichiometry (the found consumption of M referred to that calculated for the total defluorination of the precursor); δ = doping level of carbon (calculated per carbon atom also for precursors containing nitrogen). [b] In early stages of reaction K_{Na}= 0.3 nm/s, see text.

the aqueous extract (see Experimental Section). In all cases, the amount of superstoichiometric alkali metal ($M_{found} - M_{calc}$) agreed reasonably well with that found in the hydroxide MOH in reaction 5.

Precursors containing nitrogen react similarly with amalgams under complete dehalogenation (cf. eq 3) and n-doping (cf. eq 4). Elemental analysis gave the following compositions: carbonaceous material from perfluoropyridine, 61.63% C, 2.63% H, 11.91% N (N/C = 0.17); carbonaceous materials from cyanuric fluoride, 38.00% C, 2.34% H, 44.25% N (N/C = 1.00). The N/C ratios in the starting compounds, i.e., perfluoropyridine and cyanuric fluoride, are 0.20 and 1.00, respectively. The carbonaceous materials from perfluorobenzonitrile contained ca. 5−7% of extractible components which gave yellow-brown solution in water, ethanol, or acetone, and the results of elemental analysis were poorly reproducible. On the other hand, the carbons from perfluoropyridine and cyanuric fluoride gave no extractible components other than MF and MOH (cf. eqs 3 and 5), and the N/C ratio was close to that in the precursor. We may suggest that the heterocyclic nitrogen, present in the precursor, remains incorporated also in the aromatic system of the produced carbon.

3.2. Kinetics of Film Growth: Reflection Spectroscopy. The growth of carbonaceous layer produced from gaseous C_xF_y on the surface of liquid $M_{(Hg)}$ manifests itself by visual changes of the originally silvery shiny surface of $M_{(Hg)}$ after its first contact with the fluorocarbon vapor. In early stages of the film growth, the amalgam surface exhibited perfectly uniform interference colors over the whole exposed area, evidence for the uniform thickness of the film in the 10^2 nm region. The palette of interference colors repeated regularly in the sequence yellow-red-blue-green- and again yellow. Three to four orders of these colors were visible until the film became too dark for visual inspection. The perfectly uniform color (thickness) of the prime thin film over the whole exposed surface of the amalgam evidences that the growth is kinetically controlled.

Figure 1 shows an example of the UV−Vis reflection spectra of the carbonaceous film grown on top of Li amalgam after its exposure to perfluorocyclobutane vapor. For demonstration purposes, each spectrum is presented here in the color which roughly matches that of the actual film. The incident light is reflected on optically more dense media both at the C_xF_y/film and film/amalgam interfaces. Hence, the phase of incident light wave is changed by π and the intensity of reflected light (backscattered at 180°) has a minimum or maximum for thicknesses L^{min} or L^{max}, respectively

$$L^{min} = \frac{(2k - 1)\lambda}{4n_{eff}} \quad (6a)$$

$$L^{max} = \frac{k\lambda}{2n_{eff}} \quad (6b)$$

where λ denotes wavelength, $k = 1, 2, 3, ...$, and n_{eff} is the effective refractive index. Our film contains two

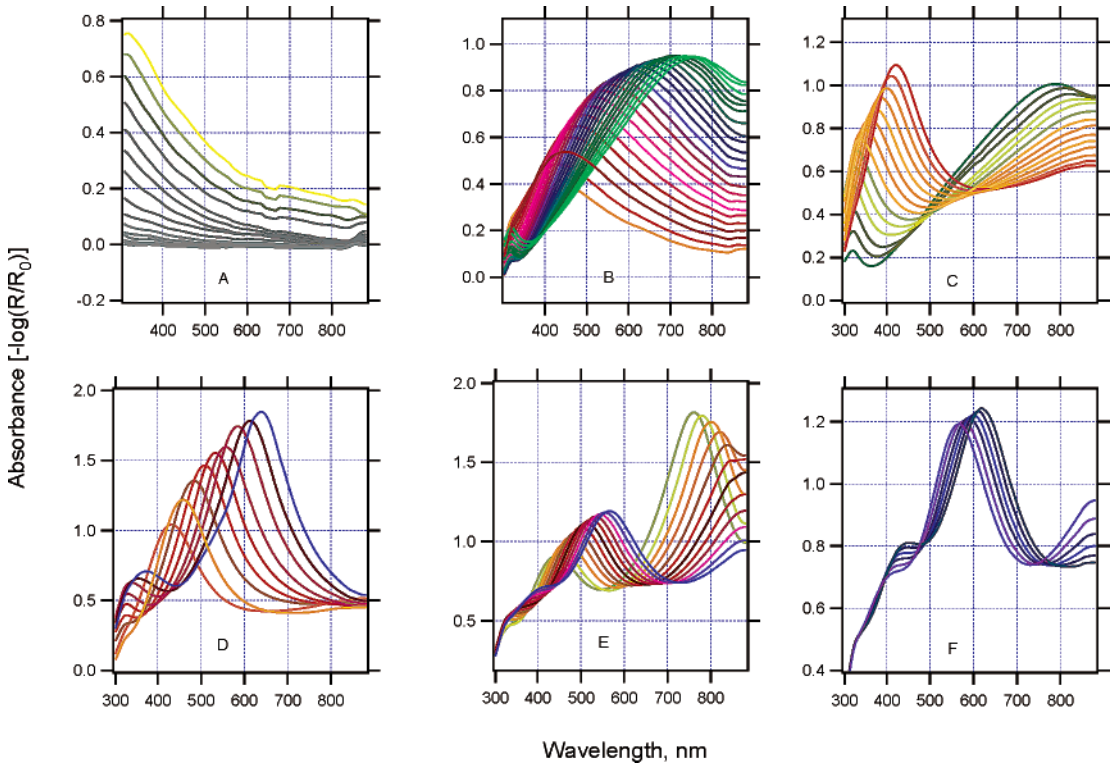

Figure 1. UV-Vis reflectance spectra of the carbonaceous film grown from perfluorocyclobutane on top of Li amalgam. The spectra were recorded in situ during the film growth at fixed time intervals: (A) reaction time 0−280 s, interval 20 s; (B) reaction time 400−840 s, interval 20 s; (C) reaction time 860−1400 s, interval 40 s; (D) reaction time 1560−2360 s, interval 100s; (E) reaction time 2740−3840 s, interval 100 s; (F) reaction time 3840−4340 s, interval 100 s.

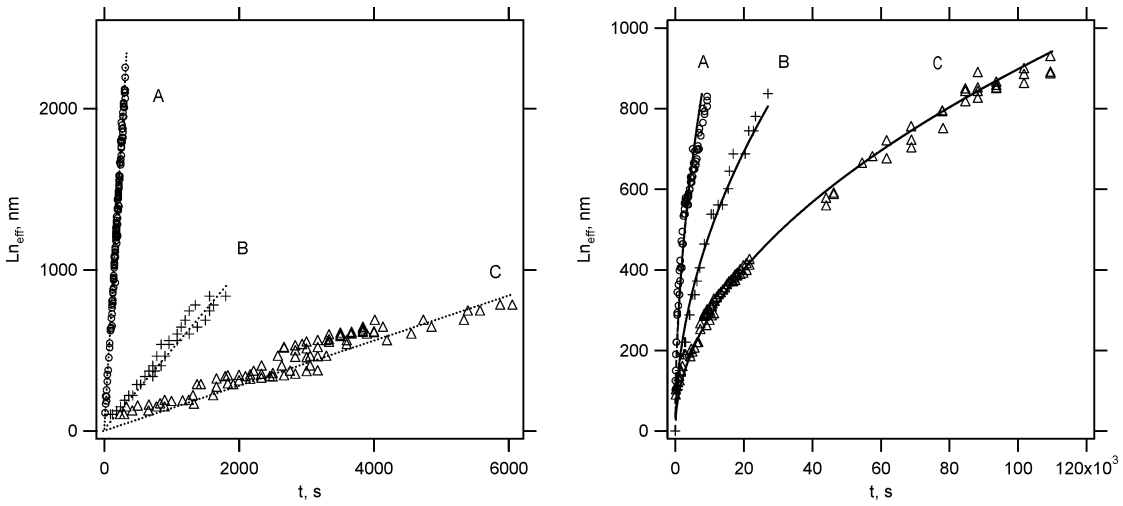

Figure 2. Effective thickness of carbonaceous layer as a function of the reaction time (t). Left panel: Reaction of Li amalgam with (A) perfluorocyclopentene, (B) perfluorodecalin, and (C) perfluoronaphthalene. Right panel: Reaction of Na amalgam with (A) perfluorocyclopentene, (B) perfluorodecalin, and (C) perfluorocyclobutane.

components: the salt MF and n-doped carbon with the corresponding refractive indexes n_1 and n_2, respectively, and the volume proportions f and $(1 - f)$, respectively. Such a composite can be approximated by an effective refractive index as follows:

$$n_{\text{eff}} = [f{n_1}^2 + (1 - f){n_2}^2]^{1/2} \qquad (7)$$

However, as n_2 is unknown, we shall further consider the film's refractive index, n_{eff} as a parameter in kinetic analysis. We further assume that the structure of the film is independent of its thickness, hence, the index n_{eff} is a constant relating the measured film thicknesses against the absolute ones.

When the film becomes thicker, its UV−Vis reflection spectrum has several interference maxima/minima satisfying the condition

$$L^{\text{min/max}} = \frac{m\lambda_1\lambda_m}{2n_{\text{eff}}(\lambda_1 - \lambda_m)} \qquad (8)$$

(m is the number of maxima/minima between the wavelengths λ_1 and λ_m).

Figure 2 shows the corresponding effective film thickness (Ln_{eff}) as a function of the reaction time for three selected precursors which reacted at 25 °C with Li amalgam (Figure 2, left panel) or Na amalgam (Figure

2, right panel). Apparently, the carbonaceous film grows linearly with time on the $Li_{(Hg)}$ surface, but linearly with the square root of the reaction time on the $Na_{(Hg)}$ surface

$$Ln_{eff} = K_{Li}t \quad (9)$$

$$Ln_{eff} = K_{Na}t^{1/2} \quad (10)$$

The rate constants K_{Li} and K_{Na} are summarized in Table 1 for various perfluorinated precursors tested. The square-root kinetics (as in eq 10) is also found for K amalgam although the film growth is very slow in this case (Table 1). According to eqs 9 and 10 the film thicknesses can be controlled simply by adjusting the reaction time. The different reaction kinetics for Li and Na or K amalgams with gaseous C_xF_y contrasts to the data for the reaction of Li, Na, or K amalgams with solid fluoropolymers.[1,6] In the latter case, eq 10 was satisfactorily valid for all these systems (i.e., also for reaction employing Li).[1,6]

To understand this inconsistency, we have suggested previously[13,17] that the overall rate of the film growth can be controlled by two processes: (i) ionic (M^+) conductivity of the growing film or (ii) intrinsic rate of the electrochemical carbonization at the interface between C_xF_y and the growing film. Depending on the actual precursor/amalgam system, either the process (i) or (ii) is the slowest one, and this dictates the overall rate of the film growth.

With $Na_{(Hg)}$ or $K_{(Hg)}$, the transport of Na^+ or K^+ controls the growth, and the kinetics is satisfactorily described by eqs 1 and 10 for all precursors. This is also valid for Li amalgam and solid fluoropolymers, but not for Li amalgam and gaseous low-molecular-weight precursors. In the latter case, the intrinsic rate of electrochemical carbonization at the interface between C_xF_y and the growing film may become slower than the transport of Li^+ through the growing film. The carbonization includes transport of gaseous molecules toward the interface, their proper orientation, anchoring at the surface, and finally reductive carbonization via electrons conducted from the Li amalgam through the film. In this case, the transport of Li^+ is faster than the rate of carbonization, and so the overall kinetics is controlled by the rate of carbonization. This is, apparently, independent of the reaction time, hence the film at the $Li_{(Hg)}$ surface grows linearly with time.

This rule is violated only for perfluoro-2-butyne, which shows the square-root dependence with $K_{Li} = 120$ nm·s$^{-1/2}$. In other words, this reaction is described by eqs 1 and 10, not by eq 9. Apparently, the rate of carbonization of perfluoro-2-butyne is so high that the reaction becomes limited by the Li^+ transport in the growing film, as in the case of Na^+/K^+ transport.

Still another exception to this simple model (eqs 9 and 10) is the reaction of perfluoronaphthalene with Na amalgam. This is documented in Figure 3. The film growth is linear at early stages of the reaction (for Ln_{eff} < 250 nm; K_{Na}= 0.3 nm/s; curve: fit_1) but becomes proportional to $t^{1/2}$ for thicker films (K_{Na}= 18 nm·s$^{-1/2}$). In other words, the Na^+ transport is rate-determining only for thicker films, but not for thinner films in this particular case.

For perfluorocyclopentene, the temperature dependence of K_{Li} was tested down to −15 °C. (Lower temperatures cannot be applied owing to small solubility of Li in mercury). The film growth slows down (cf. Table 1), but the kinetic equation (eq 9) is still valid. Qualitatively the same conclusion holds also for K_{Na} at 40 °C (eq 10 still valid). Apparently, the relative dependences of ionic conductivities and carbonization rates on temperature between −15 and 40 °C are not that significant to switch between the two rate-limiting processes.

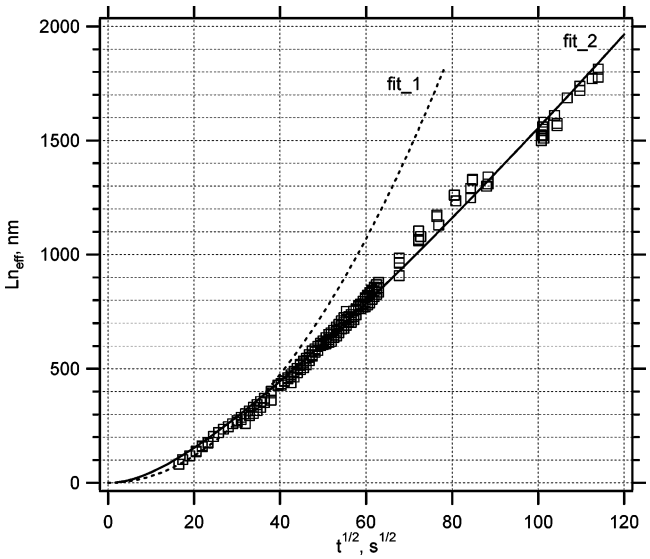

Figure 3. Kinetics of the reaction of perfluoronaphthalene with Na amalgam. Effective thickness of carbonaceous layer as a function of the square root of the reaction time ($t^{1/2}$): fit_1, $Ln_{eff} = 0.3t$; fit_2, theoretical curve, see text.

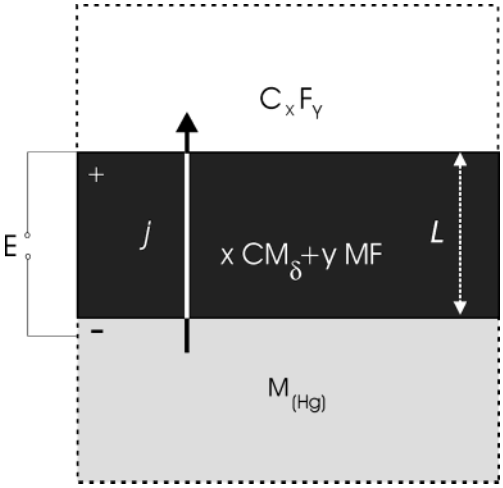

Figure 4. Scheme of the interface alkali metal amalgam, $M_{(Hg)}$ − growing film ($xCM_\delta + yMF$) − perfluorinated precursor (C_xF_y).

3.3. Kinetics of the Film growth: Theory. To rationalize the above discrepancies in experimental data on the film growth, we shall modify the classical electrochemical corrosion model by Jansta and Dousek[1,6,11] considering a planar three-layer electrochemical cell (Figure 4). The bottom layer is composed of liquid alkali metal amalgam. The top layer is a fluorocarbon precursor, C_xF_y, which may be solid, liquid, or gaseous. During the spontaneous carbonization, a corrosion layer of electrical conductivity σ ($\sigma \cong \sigma_i$) is formed on the bottom layer according to the overall reaction

$$C_xF_y + (y + x\delta)M_{(Hg)} = xCM_\delta + yMF \quad (11)$$

requiring $y + x\delta$ electrons. If a charge of $(y + x\delta)F \equiv zF$ passes, the volume, V_p, of this product mixture will be given by the equation

$$V_p = \frac{xM_C}{\rho_C} + \frac{yM_{MF}}{\rho_{MF}} \tag{12}$$

where M and ρ (with subscripts) denote molar mass and density of the respective substances. A unit volume of the product thus corresponds to a charge passed equal to zF/V_p, and in the general case, when the charge is given by a current density integral, we have

$$\int_0^t j \cdot dt = \frac{zFL}{V_p} \tag{13}$$

or in the differential form:

$$j = \frac{zF}{V_p} \cdot \frac{dL}{dt} \tag{13a}$$

Here, L denotes the thickness of the corrosion layer. Further, we introduce Ohm's law:

$$j = \frac{E\sigma}{L} \tag{14}$$

Elimination of j from the latter two equations leads to a differential equation whose solution leads to the simple time function $L(t)$

$$L = k_1\sqrt{t} \tag{15}$$

where

$$k_1 = \left(\frac{2V_pE\sigma}{zF}\right)^{1/2} \tag{16}$$

However, it is apparent that eq 14 cannot strictly apply if L approaches zero. In such a case the current is influenced by the rate of the actual electrode process, and the value of E consists of the ohmic, E_{ohm}, and activation, E_a, parts. Thus, we may write

$$j = j_0 \exp\left(\frac{\alpha z_e F E_a}{RT}\right) \tag{17}$$

where α denotes the charge-transfer coefficient and z_e is the number of electrons transferred in the rate-determining step, and further

$$j = \frac{E_{ohm}\sigma}{L} \tag{18}$$

These two equations can be combined with regard to $E = E_a + E_{ohm}$ to obtain the following:

$$E = \frac{RT}{\alpha z_e F}\ln\frac{j}{j_0} + \frac{jL}{\sigma} \tag{19}$$

By eliminating j from eqs 13 and 19 and rearranging we obtain the following differential equation that defines the model function $L = f(t)$:

$$\kappa \ln(b\eta') + c\eta\eta' = 1 \tag{20}$$

where we have introduced the dimensionless variables

$$\eta = \frac{L}{L_m},\ \eta' = \frac{d\eta}{d\xi},\ \xi = \frac{t}{t_m} \tag{21}$$

The quantities L_m and t_m denote maximum experimental values of L and t. The dimensionless coefficients are defined as

$$\kappa = \frac{RT}{\alpha z_e FE},\ b = \frac{zFL_m}{j_0V_pt_m},\ c = \frac{zFL_m^2}{EV_pt_m\sigma} \tag{22}$$

The initial condition is $\eta = 0$ for $\xi = 0$.

It can be seen that this model is more general than that in our older theory[3] since it can be applied regardless of whether the precursor is solid, liquid, or gaseous: the quantity V_p can be estimated in any case. In general, we may distinguish two limiting situations. First, for very small thickness of the corrosion layer, $\eta \ll 1$, the second term in eq 20 may be neglected, hence η' is independent of the time and we obtain simply

$$L = k_2t \tag{23}$$

with $k_2 = (L_m/bt_m)\exp(1/\kappa)$. Second, for large thickness of the corrosion layer, $\eta \sim 1$, the first term in eq 20 may be neglected and we obtain by simple integration eq 15. These rough considerations are supported by the exact solution presented below.

To solve eq 20, the first derivative, η' will be considered as an auxiliary parameter, p. First, this equation is solved with respect to η to give

$$\eta = \frac{1 - \kappa\ln(bp)}{cp} \tag{24}$$

Since obviously $d\xi = d\eta/p$ where η is given by eq 24, we can find, by integration, ξ as a function of p. The result that satisfies the above initial condition can be written as

$$\xi = \frac{1}{2cp^2}\left[1 + \frac{\kappa}{2} - \kappa\ln(bp)\right] - \frac{\kappa b^2}{4c}\exp\left(-\frac{2}{\kappa}\right) \tag{25}$$

By setting $\eta = 0$ in eq 20 we obtain the limiting value of $p = (1/b)\exp(1/\kappa) \equiv p_0$. Thus, the model function $\eta = f(\xi)$ (or $L = f(\sqrt{t})$ in practical coordinates) is given in the parametric form by eqs 24 and 25.

In fitting the experimental data for the reaction of Na amalgam with gaseous perfluoronaphthalene, an iteration procedure was developed to solve eq 25; i.e., to obtain the values of p corresponding to the chosen (experimental) values of ξ for estimated values of the parameters κ, b, and c. From these, the corresponding values of η were determined. Controlled iteration steps were employed to save the computer time. The corresponding L values were compared with the measured ones to calculate the errors.

The results are presented graphically in Figure 3 (curve fit_2) where the thickness of the reacted layer multiplied by the effective refraction index is given in nanometers as a function of the square root of the reaction time in seconds. (Here, $L_m = 2000$ nm and $\sqrt{t_m} = 120$ s$^{1/2}$.) The parameters κ, b, and c were determined from the best fit as follows: $\kappa = 0.4415$, $b = 2.588$, and

$c = 1.283$. The mean relative deviation of the fitted dependence was 0.044. (The global minimum was rather shallow). It can be seen that the model function consists roughly of two sections: the lower one suggests the linear dependence (eq 23), while the upper one approaches the parabolic dependence (eq 15). We may note that the formula for c (eq 22) can be rearranged with respect to eq 16 as $c = 2L_m^2/t_m k_1^2$. This gives a way to check the exact model against the rough one (represented by eq 15). If we approximate $L_m \cong k_1 t_m^{1/2}$, then, $c \cong 2$, while the above-mentioned exact value is $c = 1.283$.

The determination of physical parameters from the above theory depends essentially on the assumption concerning the number of electrons, z_e, transferred in the rate-determining step. With organic electrochemical systems requiring more than one electron, it is rarely assumed that $z_e > 1$ since the electrode reaction is usually complicated. This is even more so in our example of perfluoronaphthalene, which is reduced, according to eq 11, by $z = 8 + 10\delta$ electrons per molecule, where the doping parameter $\delta = 0.16$ (Table 1). The acceptance of the first electron often causes the electroactive molecule to become more reactive, so for mere orientation we shall assume that $z_e = 1$. Concerning the transfer coefficient α, the possible values are in the interval $0.1 < \alpha < 1$.

To estimate the value of V_p from eq 12, we set $x = 10$, $y = 8$, $M_C = 12.01$ g/mol, $M_{NaF} = 42.00$ g/mol, $\rho_C = 2.2$ g cm^{-3}, and $\rho_{NaF} = 2.78$ g cm^{-3}, hence $V_p = 175.5$ cm^3 mol^{-1}. From the definitions of the dimensionless parameters (eqs 22) we obtain in turn: $E = 0.0582/\alpha$ V, $j_0 = 2.83 \times 10^{-5}$ A cm^{-2}, and $\sigma = 1.96 \times 10^{-7}\alpha\ \Omega^{-1}$ cm^{-1} (the room temperature is assumed). Although the unknown value of α causes a rather large uncertainty in the calculated value of the voltage E, it is apparent that the latter is much lower than the thermodynamic value for PTFE−$Li_{(Hg)}$ reaction (3.251 V).[1] This discrepancy is due to the fact that the eight-electron reduction of perfluoronaphthalene proceeds in several reaction steps, both chemical and electrochemical, whereas the basic eq 17 refers to the first electrochemical step. The reaction steps following the first electron transfer are, presumably, faster. The analogy of this behavior with haloalkanes,[18,19] perfluorodecalin,[20] or perhalogenated polymers[21] could be pointed out.

Finally, we can compare the above exact numerical solution with the approximate one corresponding to eqs 13−16. For the maximum thickness attained, $L_m = 2$ μm, the charge passed according to eq 13 is equal to 1.056 C/cm^2, corresponding to the mean value of the current density $j = 1.056/t_m = 7.33 \times 10^{-5}$ A/cm^2. The constant k_1 in eqs 15 and 16 can be determined from the above data as 2.08×10^{-6} cm/s$^{1/2}$ giving the value of L for $t = t_m$ equal to 2.5 μm, which is close to L_m. Also the initial (i.e., the highest) current value is obtained from eq 17 for $E_a = E$ to be 2.44×10^{-4} A/cm^2, which lies above the estimated mean. Thus, the approximate theory is essentially consistent with the exact one. Also the matching of theoretical data with experimental kinetics of the film growth is satisfactory (Figures 2 and 3 and Table 1).

In summary, we have presented here a general treatment of the amalgam-driven carbonization of a palette of perfluorinated hydrocarbons. Our study upgrades the previously published data on reactions involving solid perfluorinated polymers. The carbonization method is attractive also for potential applications, as it produces self-standing carbon films at room temperature. The films are ideally flat, as they grow on the surface of a liquid amalgam (mercury) and their thickness is perfectly uniform, being self-controlled by the reaction kinetics.

Acknowledgment. This work was supported by the Academy of Sciences of the Czech Republic (contract A4040306).

CM049116A

(18) Savéant, J. M. *Tetrahedron* **1994**, *50*, 10117.
(19) Savéant, J. M. *J. Phys. Chem.* **1994**, *98*, 3716.
(20) Combellas, C.; Kanoufi, F.; Thiébault, A. *J. Phys. Chem. B* **2003**, *107*, 10894.
(21) Combellas, C.; Ghilane, J.; Kanoufi, F.; Mazouzi, D. *J. Phys. Chem. B* **2004**, *108*, 6391.